INTERNATIONAL JOURNAL OF MEDICAL SCIENCE AND DENTAL HEALTH
(ISSN: 2454-4191)
www.ijmsdh.org (2026)

Received: 12 July 2026
Revised: 28 July 2026
Accepted: 28 Aug 2026
Published: 23 Sep 2026

Volume 12 Issue 09, 2026
Page No - 211-221
DOI - 10.55640/ijmsdh-12-09-25

Article Citation: Togboyev Komil Tuymurodovich, & Tuksanova Nasiba Esanovna. (2026). Morphometric and Histochemical Changes in The Liver After Standard and Glucocorticoid (Hormonal) Therapy of Post-Abdominal-Surgery Scars: An Experimental Study. International Journal of Medical Science and Dental Health, 12(09), 211-221. https://doi.org/10.55640/ijmsdh-12-09-25

Morphometric and Histochemical Changes in The Liver After Standard and Glucocorticoid (Hormonal) Therapy of Post-Abdominal-Surgery Scars: An Experimental Study

Togboyev Komil Tuymurodovich

Associate Professor, Department of Anatomy and Clinical Anatomy, Bukhara State Medical Institute named after Abu Ali ibn Sina, Bukhara, Uzbekistan

Tuksanova Nasiba Esanovna

Associate Professor, Department of Anatomy and Clinical Anatomy, Bukhara State Medical Institute named after Abu Ali ibn Sina, Bukhara, Uzbekistan

Abstract

Background. Glucocorticoids are widely used to treat pathological post-surgical scars, yet the morphological consequences of such therapy for the liver are not well defined.

Objective. To compare the morphometric and histochemical state of the liver in a rat model of post-abdominal-surgery scarring under standard (conventional) therapy versus glucocorticoid (hormonal) therapy, relative to healthy controls.

Methods. 140 outbred rats were allocated to control, standard-therapy and hormonal-therapy groups. Liver samples were stained with haematoxylin–eosin, Van Gieson, Masson trichrome and Alcian blue. Vascular and cellular structures were measured by digital morphometry; fibrosis, collagen, mucopolysaccharides, sinusoidal change and platelet aggregation were graded semi-quantitatively (0–10). Data are M±m; $P<0.05$ was significant.

Results. Standard therapy produced marked hypertrophic-inflammatory change: Kupffer cells rose from 11 to 59 (+436%), binucleate hepatocytes from 4.5 to 14 (+211%), central-vein diameter from 54.0 to 59.8 µm, with high histochemical scores (Van Gieson fibrosis 8, Masson collagen 9, Alcian mucopolysaccharides 9) and platelet aggregation (63 platelets/678 px²). Hormonal therapy shifted every indicator

toward control values: Kupffer cells 21, binucleate hepatocytes 5, central vein 56.0 µm, mean histochemical score falling from 6.4/5.0/4.8 to 2.0/2.0/1.8, with no platelet aggregation (11 platelets/324 px²).

Conclusion. Standard therapy aggravated hepatic inflammation, hypertrophy, fibrosis and microthrombosis, whereas glucocorticoid therapy attenuated these changes by 3–4-fold and restored a near-normal hepatic architecture, supporting a pathogenetically justified, hepatoprotective role for hormonal therapy under the studied conditions.

Keywords: Liver; morphometry; histochemistry; glucocorticoid therapy; hepatic fibrosis; Kupffer cells; post-surgical scar; experimental model.

1. Introduction

Postoperative peritoneal adhesions and pathological scarring are among the most frequent and costly complications of abdominal surgery, driven by a transforming growth factor-β (TGF-β)-centred fibrogenic programme. Intralesional glucocorticoids are a mainstay of pathological scar management, reducing collagen and glycosaminoglycan synthesis, fibroblast proliferation and inflammatory mediators. Because the liver is the principal organ of drug metabolism and a major site of fibrogenesis mediated by hepatic stellate cells, systemic exposure to hormonal agents may affect hepatic morphology in either direction — anti-fibrotic or hepatotoxic.

Despite the biological plausibility of a hepatic response to hormonal scar therapy, direct morphological evidence is scarce. The present study therefore quantifies, in an experimental rat model, the morphometric and histochemical state of the liver under standard versus glucocorticoid therapy of post-abdominal-surgery scarring, benchmarked against healthy controls.

2. Methods

2.1. Animals and groups

A total of 140 sexually mature outbred (5-month-old) rats were kept under standard vivarium conditions (humidity 50–60%, temperature 19–22 °C, 12/12 h light cycle) and randomly allocated to three groups: (i) control — healthy, untreated animals (physiological reference); (ii) standard-therapy — scar disease treated by the conventional protocol; (iii) hormonal-therapy — scar disease treated with glucocorticoids. All procedures complied with institutional bioethical requirements for the humane handling of laboratory animals.

2.2. Histological and histochemical processing

Liver tissue (whole-organ macro-specimen and samples from different lobes) was fixed, paraffin-embedded and sectioned at 4–5 µm. Sections were stained with haematoxylin–eosin (H&E) for general architecture, Van Gieson and Masson trichrome for collagen, and Alcian blue for acid mucopolysaccharides. Microphotographs were captured with a digital microscope at ×100–×1000.

2.3. Morphometry and semi-quantitative scoring

Diameters of the central vein, interlobular veins and arteries, bile ducts and sinusoidal capillaries, together with Kupffer-cell and binucleate-hepatocyte counts (per standardised pixel area), were measured on digitised images. Fibrosis, collagen accumulation, mucopolysaccharide content, sinusoidal change and platelet aggregation were graded on a 0–10 ordinal scale for each stain; the mean, standard deviation and range were computed per stain.

2.4. Statistical analysis

Results are expressed as arithmetic mean ± standard error (M±m). Between-group differences were assessed with the Student (t) and Fisher (F) criteria; a probability of $P<0.05$ was considered statistically significant.

3. Results

3.1. Standard therapy: morphometry versus control

In the control group the liver displayed normal architecture: radially arranged hepatocyte plates, orderly sinusoids and preserved portal triads (Figure 1). After standard therapy, the liver showed pronounced hypertrophic and inflammatory change — intravascular congestion, leukocytic infiltration and sinusoidal dilatation (Figure 4). Morphometrically, all indicators increased relative to control (Table 1, Figures 2–3). The most striking changes were a rise in Kupffer cells from 11 to 59 (+436%) and in binucleate hepatocytes from 4.5 to 14 (+211%); central-vein diameter increased from 54.0 to 59.8 µm and liver mass from 15.5 to 17.4 g (all $P<0.05$).

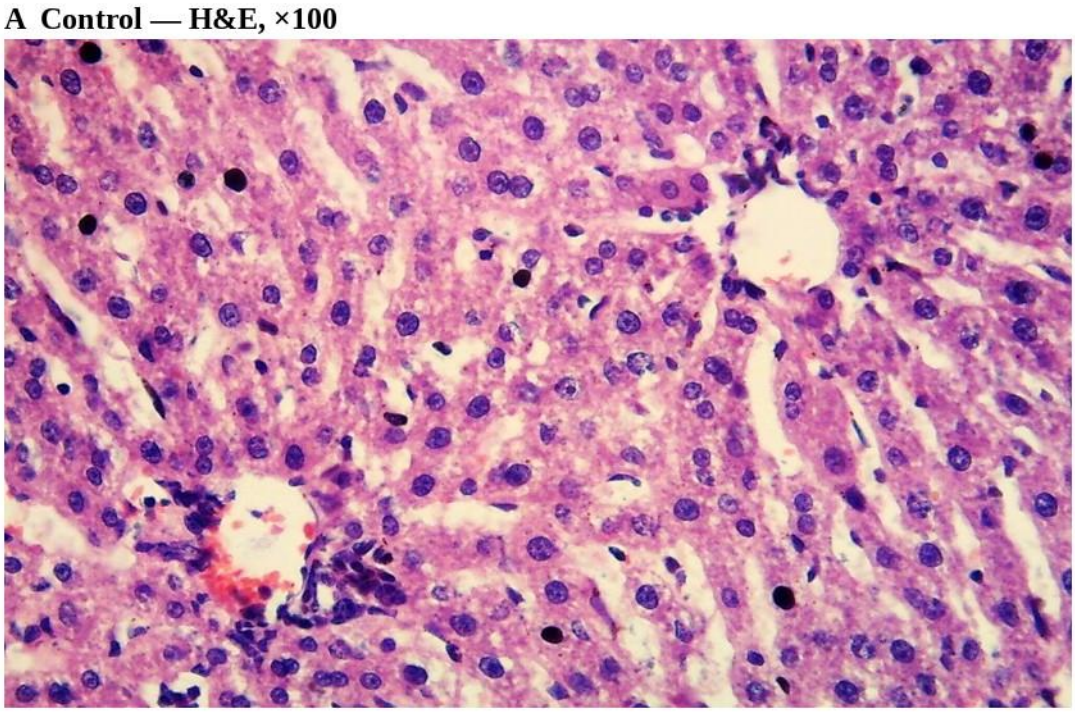

Figure 1. Control group. H&E, ×100. Normal lobular architecture: 1 — portal triad; 2 — central vein; 3 — hepatocytes; 4 — sinusoids and Kupffer cells.

Table 1. Morphometric changes after standard therapy versus control (M±m).

No.	Indicator	Control	Standard therapy	Δ %
1	Liver mass (g)	15.5±0.32	17.4±0.47	+12
2	Liver volume (ml)	22.6±0.59	24.9±0.56	+10
3	Central vein diameter (μm)	54.03±1.86	59.82±1.14	+11
4	Interlobular veins (μm)	87.8±1.75	91.3±1.13	+4
5	Interlobular arteries (μm)	25.62±0.68	30.13±0.55	+18
6	Sinusoidal capillaries (μm)	28.36±0.78	30.92±0.41	+9
7	Kupffer cells	11.0±0.31	59.0±1.16	+436
8	Binucleate hepatocytes	4.5±0.11	14.0±0.34	+211

Figure 2. Vascular morphometry: control vs standard therapy

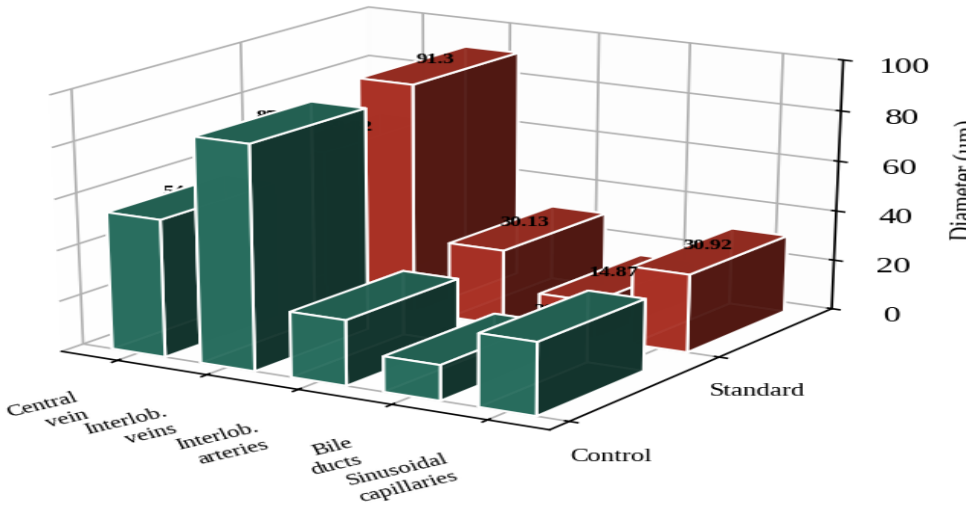

Figure 2. Vascular structure diameters (µm): control vs standard therapy. Editable 3-D chart: Excel sheet "T1-Ctrl-vs-Standard".

Figure 3. Kupffer & binucleate hepatocytes: control vs standard

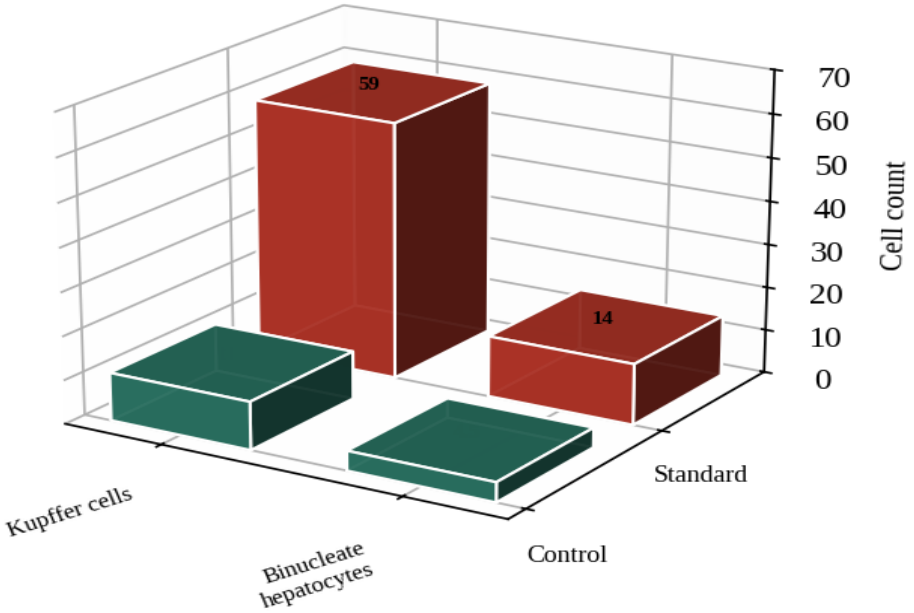

Figure 3. Kupffer cells and binucleate hepatocytes: control vs standard therapy.

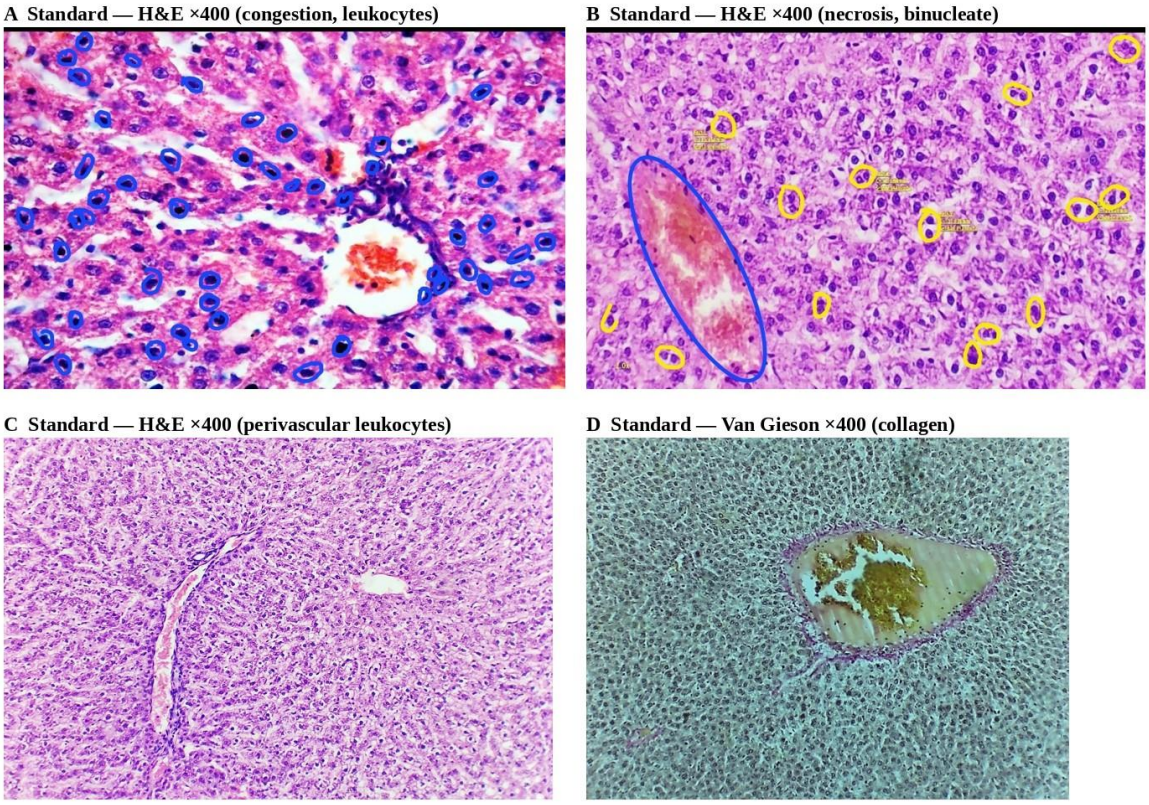

Figure 4. Standard therapy, H&E. (A) ×400 central-vein congestion and leukocytic infiltration; (B) ×400 anuclear (necrotic) and binucleate hepatocytes; (C) ×400 perivascular leukocyte accumulation; (D) ×400 Van Gieson — central vein with collagen.

3.2. Standard therapy: histochemical scoring

Histochemistry confirmed active fibrogenesis under standard therapy. Van Gieson highlighted periportal collagen and a central-vein platelet count of 63 per 678 px² with clear adhesion and aggregation; Masson revealed portal-tract connective-tissue expansion; and Alcian blue showed focal mucopolysaccharide accumulation, indicating a persistent exudative component (Figure 6). Semi-quantitative scoring (Table 2, Figure 5) yielded high values — Van Gieson fibrosis 8 and platelet 9, Masson collagen 9, Alcian mucopolysaccharides 9 — with mean scores of 6.4, 5.0 and 4.8 respectively.

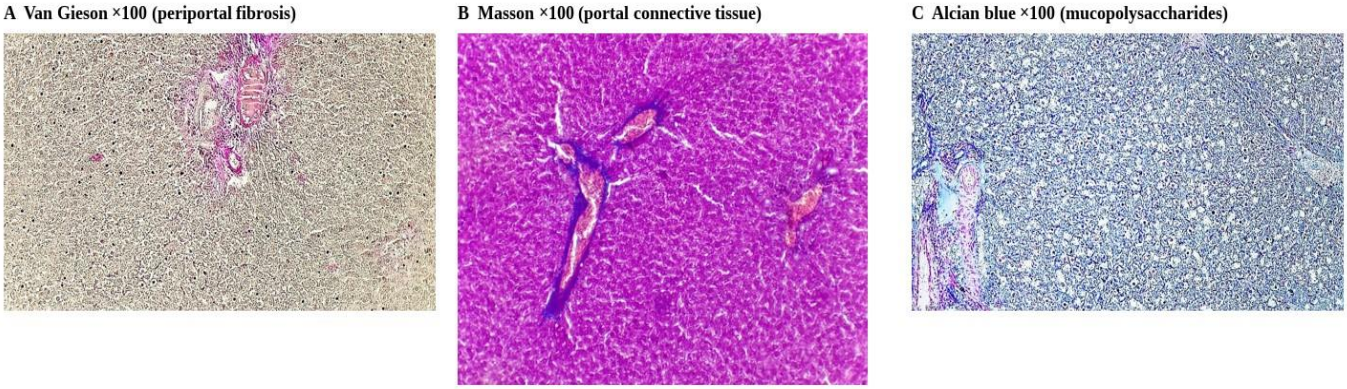

Figure 6. Standard therapy, histochemistry. (A) Van Gieson ×100 — periportal fibrosis; (B) Masson ×100 — portal connective tissue; (C) Alcian blue ×100 — mucopolysaccharides.

Table 2. Semi-quantitative histochemical scoring — standard therapy (0–10).

Stain	Fibrosis	Collagen	MPS	Sinusoid	Platelet	Mean
Van Gieson	8	7	2	6	9	6.4
Masson	7	9	3	5	1	5.0
Alcian blue	3	4	9	6	2	4.8

Figure 5. Semi-quantitative histochemical scoring — standard therapy

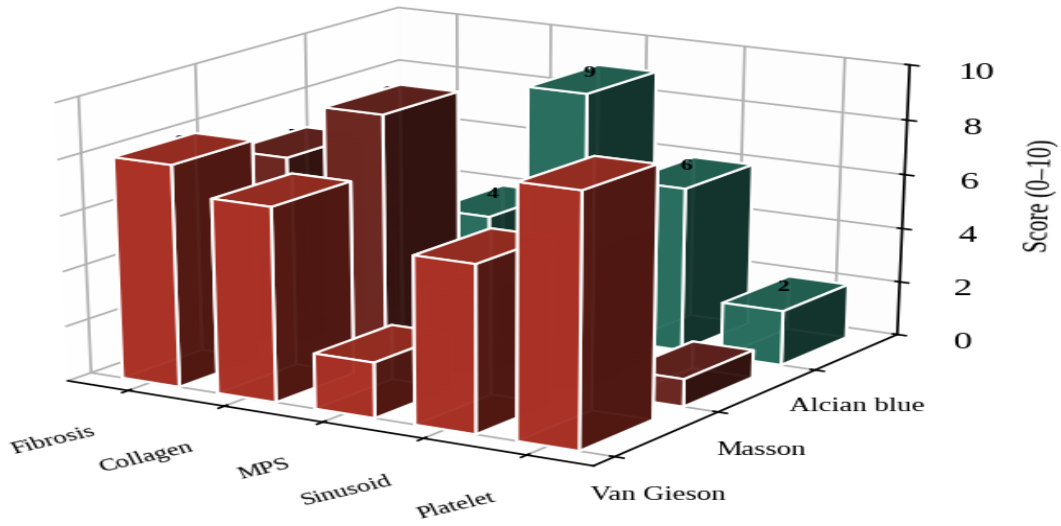

Figure 5. Semi-quantitative histochemical scoring under standard therapy. Editable 3-D chart: Excel sheet "T2-Score-Standard".

3.3. Hormonal therapy: morphometry versus standard and control

Under hormonal therapy the hepatic picture approached normal. H&E showed reduced congestion, fewer necrotic (anuclear) hepatocytes and a fall in Kupffer cells to 21 and binucleate hepatocytes to 5 (Figure 9). Across three groups (Table 3, Figures 7–8), hormonal-therapy values consistently lay between control and standard — central vein 56.0 µm, interlobular arteries 27.8 µm, liver mass 16.1 g — i.e., the pathological hyperplasia of standard therapy was largely averted. Portal-tract structures were well differentiated and mineral microvascular flow appeared stable.

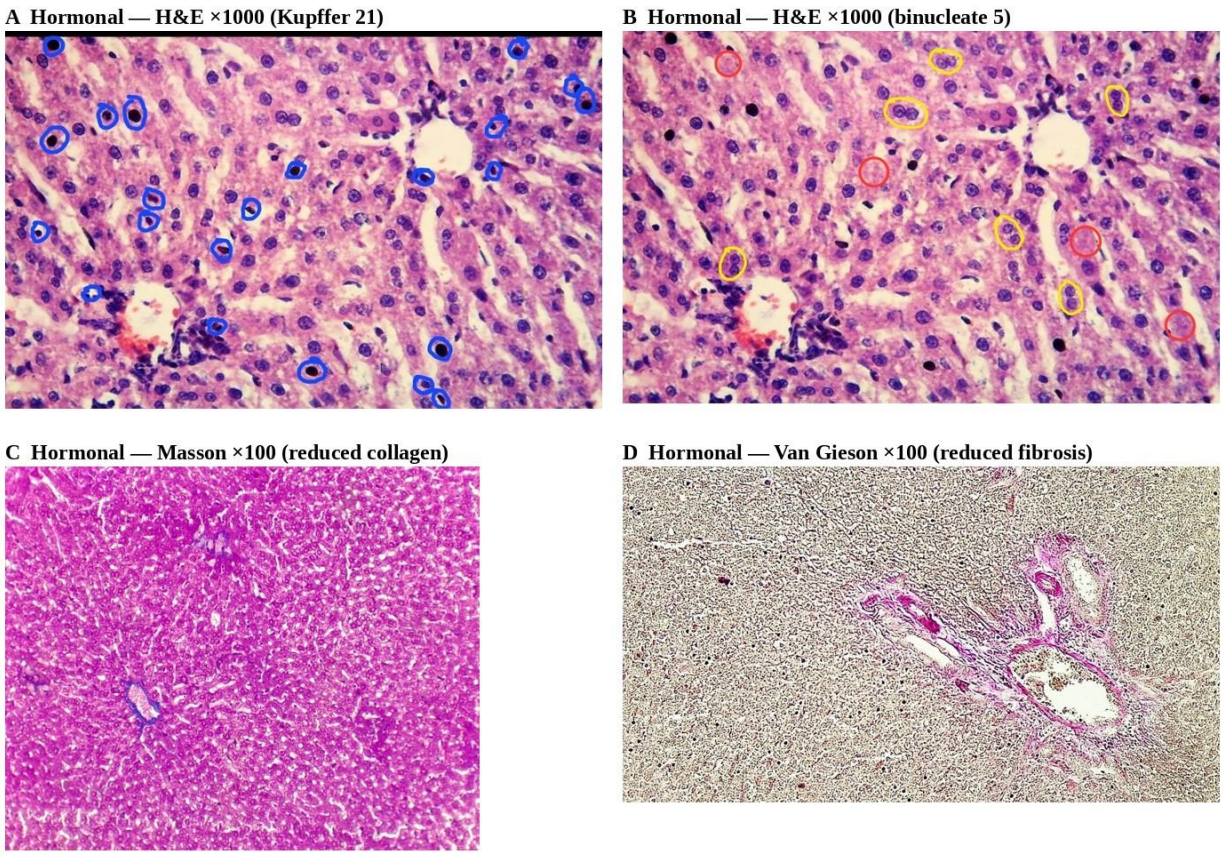

Figure 9. Hormonal therapy. (A) H&E ×1000 — Kupffer cells reduced to 21; (B) H&E ×1000 — binucleate hepatocytes reduced to 5; (C) Masson ×100 — reduced pericentral collagen; (D) Van Gieson ×100 — reduced periportal fibrosis.

Table 3. Morphometry across control, standard and hormonal therapy (mean values).

No.	Indicator	Control	Standard	Hormonal
1	Liver mass (g)	15.5	17.4	16.1
2	Central vein diameter (µm)	54.03	59.82	56.02
3	Interlobular arteries (µm)	25.62	30.13	27.79
4	Sinusoidal capillaries (µm)	28.36	30.92	29.88
5	Kupffer cells	11.0	59.0	21.0
6	Binucleate hepatocytes	4.5	14.0	5.0

Figure 7. Vascular morphometry — three groups

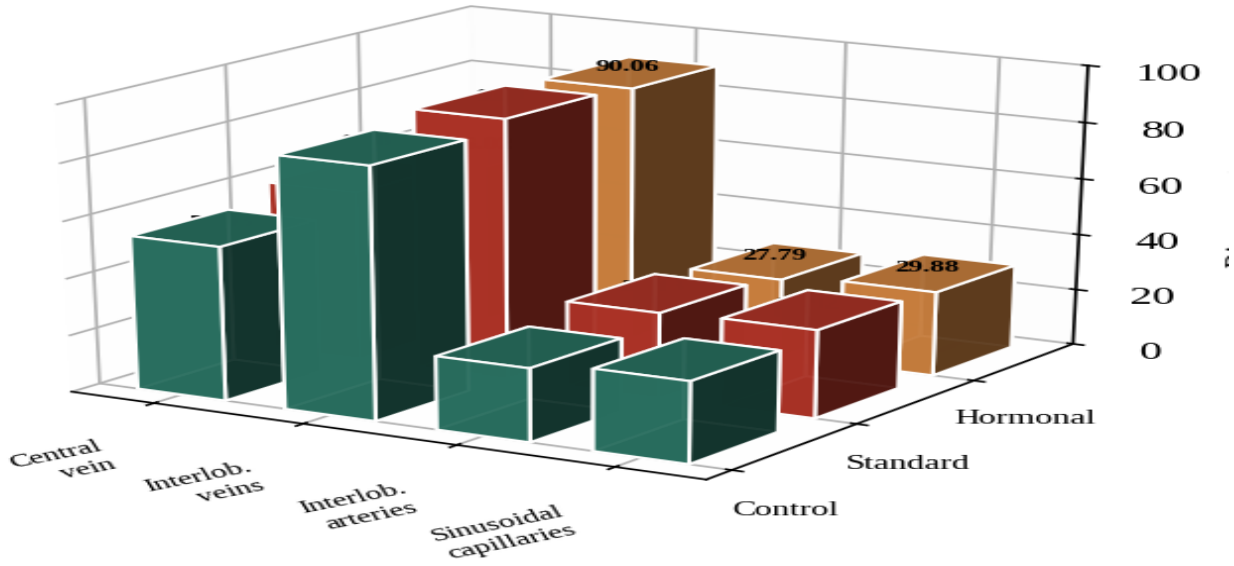

Figure 7. Vascular structure diameters (µm) across three groups. Editable 3-D chart: Excel sheet "T3-Three-groups".

Figure 8. Kupffer & binucleate hepatocytes — three groups

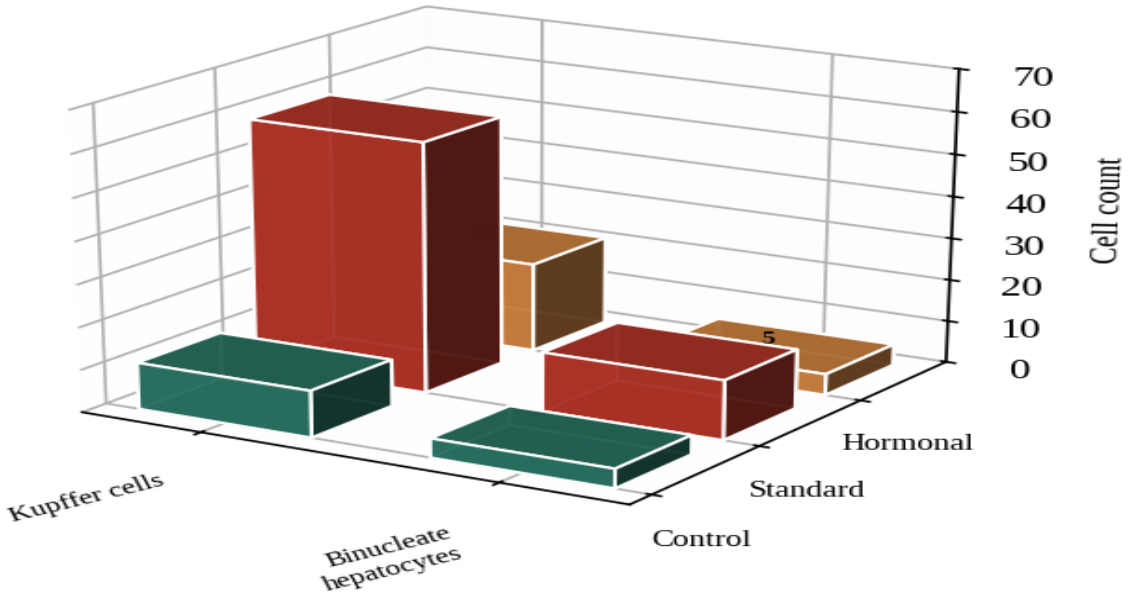

Figure 8. Kupffer cells and binucleate hepatocytes across three groups.

3.4. Hormonal therapy: histochemical scoring and platelet status

Hormonal therapy sharply reduced fibrogenic and exudative activity. Collagen deposition (Masson, Van Gieson)

and mucopolysaccharides (Alcian blue) were weakly expressed, and no platelet aggregation was observed — only 11 platelets per 324 px² versus 63 per 678 px² under standard therapy (Table 5). Mean histochemical scores fell from 6.4/5.0/4.8 (standard) to 2.0/2.0/1.8 (hormonal), a 3–4-fold reduction (Table 4, Figure 10). The integrated three-group comparison (Figure 11) shows standard therapy at the peak of pathological hyperplasia and hormonal therapy restoring near-normal values.

Table 4. Semi-quantitative histochemical scoring — hormonal therapy (0–10) and comparison of mean scores.

Stain	Fibrosis	Collagen	MPS	Mean (hormonal)	Mean (standard)
Van Gieson	3	2	2	2.0	6.4
Masson	3	2	2	2.0	5.0
Alcian blue	2	2	2	1.8	4.8

Figure 10. Mean histochemical score — standard vs hormonal

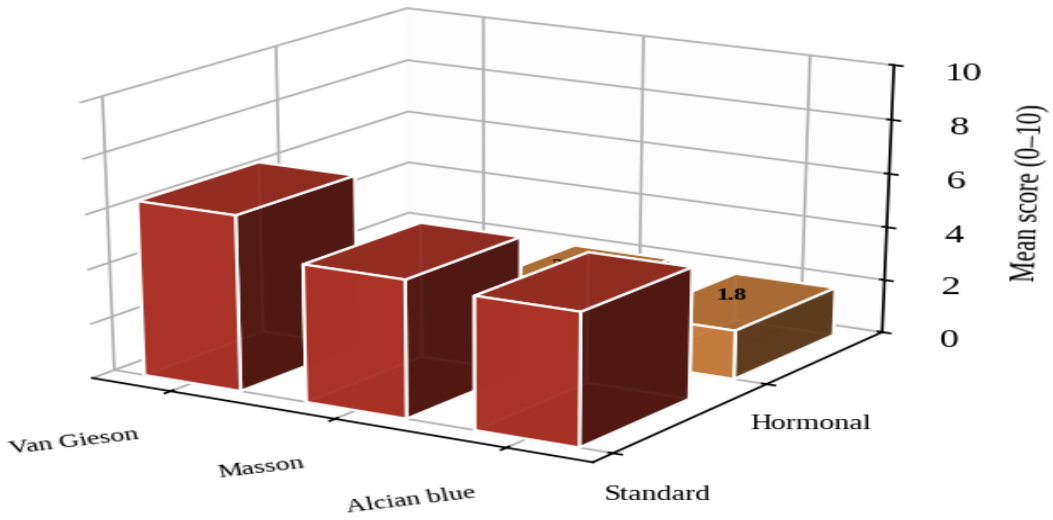

Figure 10. Mean histochemical score: standard vs hormonal therapy. Editable 3-D chart: Excel sheet "T4-Score-Hormonal".

Table 5. Platelet count and aggregation.

Group	Area (px²)	Platelet count	Aggregation
Standard (Van Gieson)	678	63	Present
Hormonal (H&E)	324	11	Absent

Figure 11. Key indicators across three groups

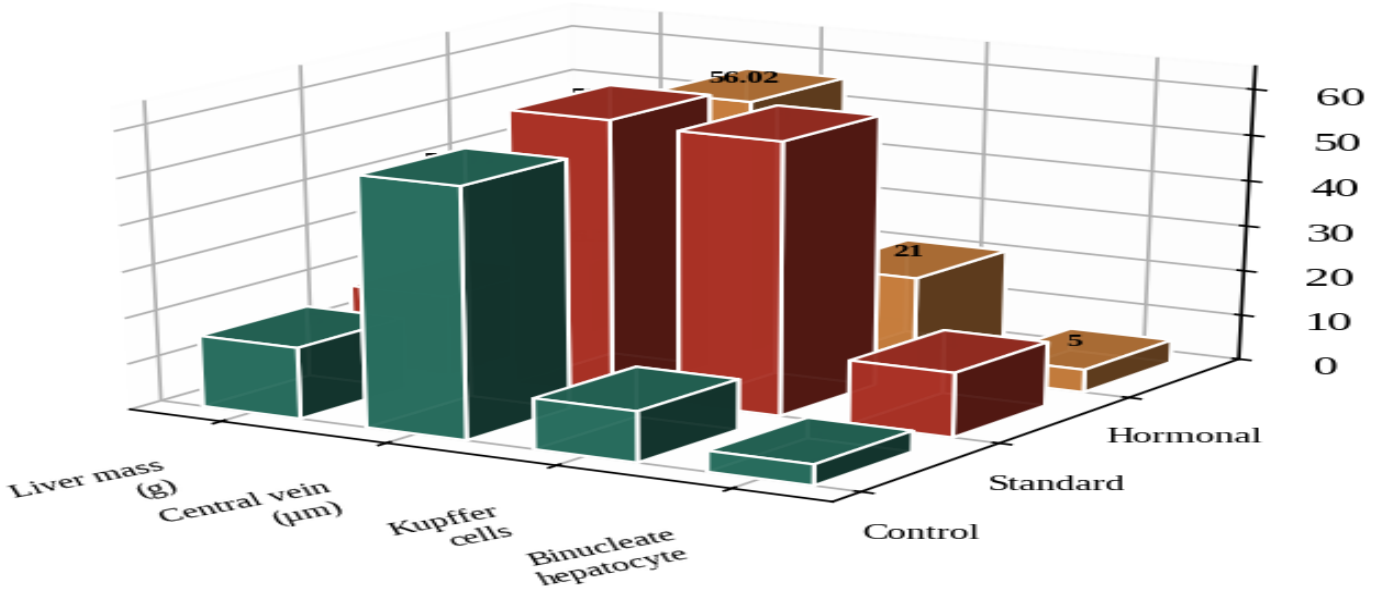

Figure 11. Key indicators across the three groups (integrated comparison). Editable 3-D chart: Excel workbook "Article2_Results_figures.xlsx".

4. Discussion

The present findings show that the two therapeutic strategies affect the liver in opposite directions. Standard therapy did not protect the organ; instead it intensified hypertrophic, inflammatory, fibrotic and microthrombotic processes, as evidenced by a near five-fold rise in Kupffer cells, a tripling of binucleate hepatocytes and high histochemical fibrosis/collagen/mucopolysaccharide scores. These changes are consistent with a TGF-β-driven fibrogenic response in which activated hepatic stellate cells deposit type I and III collagen and α-smooth-muscle actin, the hallmark of progressive hepatic fibrogenesis described in recent bibliometric and mechanistic analyses.

Hormonal (glucocorticoid) therapy, by contrast, moved every morphometric and histochemical indicator back toward control values and abolished platelet aggregation. This is concordant with experimental evidence that glucocorticoids exert cell-type-specific, largely anti-inflammatory and anti-fibrotic effects through the glucocorticoid receptor in hepatic stellate and immune cells, including up to ~60% reduction of hepatic α-smooth-muscle actin in cholestatic models and antagonism of the TGF-β–Smad3 axis via co-regulation of PAI-1 and connective-tissue growth factor. The 3–4-fold reduction of mean histochemical scores observed here (6.4/5.0/4.8 → 2.0/2.0/1.8) provides direct morphological confirmation of this anti-fibrotic capacity in the setting of post-surgical scar therapy.

These results must be weighed against the recognised hepatotoxic potential of systemic pharmacotherapy: drug-induced liver injury occurs in ~14–19 per 100,000 persons annually and accounts for roughly 11% of acute liver failure. In the present model, however, the net hepatic effect of glucocorticoids was protective rather than injurious, suggesting that under controlled dose and duration the anti-fibrotic benefit predominates. The histochemical toolkit used here — Van Gieson, Masson and Alcian blue with 0–10 semi-quantitative scoring — is well validated for fibrosis assessment, although semi-quantitative Masson scoring is known to be less reproducible than digital collagen-proportionate-area analysis, which should complement ordinal scoring in future work.

Study strengths include the three-group design, combined morphometric–histochemical assessment and a large animal cohort. Limitations include the observer-dependence of ordinal scoring and the absence of immunohistochemical markers (α-SMA, CD68, TGF-β); their addition, together with digital image analysis and dose–response evaluation, would further strengthen causal inference.

5. Conclusion

In an experimental rat model of post-abdominal-surgery scarring, standard therapy aggravated hepatic inflammation, hypertrophy, fibrosis and microthrombosis, whereas glucocorticoid (hormonal) therapy attenuated these changes 3–4-fold and restored a near-normal hepatic architecture and microcirculation. Morphometric indicators under hormonal therapy consistently lay between control and standard values, indicating avoidance of pathological hyperplasia. These findings support a pathogenetically justified, hepatoprotective role for glucocorticoid therapy under the studied conditions and warrant confirmation with immunohistochemical and digital-morphometric methods and clinical correlation.

References

1. Yang L, Fang Y, Lian Y, et al. Aloe-emodin targeting FOXC2 disrupts NETs formation and EMT-driven postoperative peritoneal adhesion through the TGF-β1–Smad2/3 pathway. Adv Sci. 2025. doi:10.1002/advs.202511013.
2. Tabibian N, et al. Postoperative peritoneal adhesion: an update on physiopathology and modern therapeutics. Naunyn Schmiedebergs Arch Pharmacol. 2020;393:1387–1408.
3. From mechanisms to anti-fibrotic drugs in hepatic stellate cell research: a global bibliometric analysis (2000–2025). Front Pharmacol. 2025. doi:10.3389/fphar.2025.1734449.
4. Tacke F, Trautwein C. Mechanisms of liver fibrosis resolution. J Hepatol. 2015;63(4):1038–1039.
5. Hernandez-Gea V, Friedman SL. Pathogenesis of liver fibrosis. Annu Rev Pathol. 2011;6:425–456.
6. Glucocorticoids have opposing effects on liver fibrosis in hepatic stellate and immune cells. Mol Endocrinol. 2016;30(8):905–917.
7. Glucocorticoids cause gender-dependent reversal of hepatic fibrosis in the MDR2-knockout mouse model. Int J Mol Sci. 2017;18(12). PMCID: PMC5713358.
8. Weiler SME, et al. Glucocorticoids activate TGF-β-induced PAI-1 and CTGF expression in rat hepatocytes. PMCID: PMC1868771.
9. Acharya R, et al. Efficacy and safety of intralesional triamcinolone acetonide alone and with 5-fluorouracil in keloids and hypertrophic scars: a randomised trial. Skin Health Dis. 2024;4(5):e450.
10. Li X, et al. Incidence and risk factors of drug-induced liver injury. Liver Int. 2022;42(9):1999–2014.
11. Insights into medication-induced liver injury: understanding and management strategies. 2024. PMCID: PMC11928981.
12. Husain N, Hamdan AR. Quantitative histomorphometric analysis of collagen bundles in Masson's trichrome-stained rat skin. Health Sci Rep. 2026;9:e71998.
13. Standish RA, et al. Comparison of histochemical stainings in the evaluation of liver fibrosis. 2015. PMCID: PMC4664783.
14. Usanov SS. Morphometric characteristics of the liver in outbred rats. 2023;98–105.